Grinding of Cemented Carbide Using a Vitrified Diamond Pin and Lubricated Liquid Carbon Dioxide

Strojniški vestnik - Journal of Mechanical Engineering 69(2023)11-12, 435-443
DOI:10.5545/sv-jme.2023.658
Original Scientific Paper
Received for review: 2023-05-27
Received revised form: 2023-09-12
Accepted for publication: 2023-10-04

Grinding of Cemented Carbide Using a Vitrified Diamond Pin and Lubricated Liquid Carbon Dioxide

Deepa Kareepadath Santhosh[1,*] – Franci Pušavec[1] – Peter Krajnik[1,2]
[1] University of Ljubljana, Faculty of Mechanical Engineering, Slovenia
[2] Chalmers University of Technology, Department of Industrial and Materials Science, Sweden

Despite extensive research on grinding of cemented carbide, few studies have examined abrasive machining of this material using small-diameter super abrasive tools (also known as grinding pins/points), especially with respect to varying cooling-lubrication methods. This study therefore focuses on a comparative experimental investigation of three such methods - dry, emulsion, and lubricated liquid carbon dioxide (LCO_2-MQL). The performance of these methods and the resulting grindability are examined in terms of grinding forces, force ratios, specific energy, and through the analysis of wheel loading. The results show that LCO_2-MQL grinding has lower grinding forces (normal forces – 8 % to 145 % lower than dry grinding, and 18 % to 33 % lower than emulsion grinding and tangential forces – 4 % to 66 % lower than dry grinding and 28 % to 78 % lower than emulsion grinding) and specific energy 24 % to 51 % lower compared to dry grinding and 64 % to 69 % lower than emulsion grinding, indicating its potential for efficient material removal. However, a challenge with high wheel loading was observed with LCO_2-MQL, likely due to the lack of oxygen in the CO_2 grinding atmosphere. Despite this issue, the LCO_2-MQL method shows potential for efficient operations, especially at higher aggressiveness values where the lowest specific energies were achieved. These results provide new insights into various aspects of cooling-lubrication methods in the pin grinding of cemented carbides.
Keywords: diamond, grinding, cemented carbides, cooling-lubrication, carbon dioxide

Highlights
- *Analysis of different cooling-lubrication conditions reveals LCO_2-MQL as a potentially superior method.*
- *LCO_2-MQL reduces grinding forces and specific energy in pin grinding.*
- *LCO_2-MQL achieves the lowest force ratio, indicating superior lubrication capability.*
- *Wheel loading is present in all cooling-lubrication methods but is most severe in LCO_2-MQL.*

0 INTRODUCTION

Cemented carbides, known for their excellent combination of hardness, wear resistance, and toughness, have become the most common cutting tool materials for machining applications. The combination of the high hardness of tungsten-carbide (WC) grains cemented into a composite by a ductile Co binder yields outstanding mechanical properties [1]. Cemented carbides are considered hard-to-machine materials due to their high strength at elevated temperatures and low modulus of elasticity [2]. This work focuses on the GC1130 grade developed by Sandvik Coromant, which features a high hardness and wear-resistant substrate due to its high chromium content and fine-grained microstructure. The WC grain boundaries are structured to enhance edge toughness, and the grade is designed to resolve tool life and issues associated with chipping, flaking, and thermal cracking in milling operations.

Due to its inherent hardness, the production of cemented carbides almost always includes grinding using diamond grinding wheels at the end of the manufacturing value chain. Diamond wheels typically feature a metal bond, or a hybrid, resinoid-metal, bond. The grinding of cemented carbides is in high demand in the industry, and these processes are accompanied by high grinding forces, specific energy, wheel wear, and low material removal rates [3]. Another concern, common on the shop floor but not extensively researched, is wheel loading, which is especially challenging when grinding with low aggressiveness. In a loaded wheel, the workpiece material becomes embedded within the pores of the diamond wheel, which prevents normal grinding action, i.e., material-removal by chip formation. Badger reported that loading of cemented carbide workpiece material does not appear to be caused by the high ductility of the workpiece material or a chemical reaction, but rather by the short, WC-Co chips [4]. The author proposed the loading be removed via stick-conditioning. In production, grinding machines have conditioning (sticking) done by truing using aluminum oxide wheels, often used in-process while grinding. In some cases, an external truing wheel can be used [5]. In the most challenging applications, diamond-wheel conditioning is done on metal-bonded wheels by spark electric-discharge dressing, which requires a special wheel design and grinding fluid to facilitate electrical conductivity [6].

Grinding fluids reduce the friction in the contact between the tool and the workpiece. This is achieved

*Corr. Author's Address: University of Ljubljana, Faculty of Mechanical Engineering, Aškerčeva 6, 1000 Ljubljana, Slovenia, deepa.kareepadathsanthos@fs.uni-lj.si

through lubrication. Grinding fluids also dissipate heat from the grinding zone, i.e., they provide cooling. While most industrial grinding of cemented carbides is done using (petroleum-based) straight oils, it is also possible to use a solution synthetic fluid, which is considered more environmentally friendly due to the large proportion of water (e.g., 95 %) in the grinding fluid. Both types of grinding fluids typically contain additives, such as chemical substances to inhibit cobalt leaching, i.e., removal of the cobalt binder. To further improve sustainability, it is viable to drastically reduce the amount of grinding fluids used [7]. For example, minimum quantity lubrication (MQL) technology can be used in the grinding of cemented carbides, which employs an oil-mist to lubricate the grinding process at a consumption rate that is on a mL/hour scale [8]. Nevertheless, while MQL can lubricate the process, it has limited cooling capability [9]. Therefore, recent innovative solutions include using subcooled MQL, for example, by using liquid nitrogen to reduce the temperature of the MQL oil mist [10], or by dissolving the oil in liquid carbon dioxide (LCO_2), which upon exiting a nozzle drops to a temperature of −78.5 °C and freezes the oil droplets, which measure only 2 micrometers in diameter [11]. Such advanced solutions to cooling and lubrication have not yet been explored in the grinding of cemented carbides. This work focuses on investigating the LCO_2 solution, as this technology has proven superior in other machining applications, such as in drilling [12] and milling [13]. Even though the pressure in LCO_2 cylinder is nearly 6 MPa (60 bar), it is likely that the air barrier formed around a grinding wheel rotating at high speed would prevent the LCO_2 from entering the grinding zone and causing it to be diverted elsewhere. Therefore, the first grinding investigation using LCO_2 intentionally involved using a tool with a much smaller diameter that does not create a distinct air barrier and is hence a lower obstacle to gas/oil-mist penetration. In conventional grinding, wheel diameters typically measure 400 mm to 600 mm, whereas the diameter of the grinding pins in focus here was only 6 mm. Grinding with small (generally ≤15 mm) fixed-abrasive tools, such as diamond pins mounted on a high-speed machining center is often referred to as pin or point grinding [14], which has proven to be a capable process for machining of hard and brittle materials with high dimensional accuracy and fine surface finish demands [15], due to a small grit-penetration depth. The available research on pin grinding of cemented carbides is limited. Kadivar et al. [16] studied the process mechanics and surface integrity of micro-grinding of titanium alloys and ceramics. Arrabiyeh et al. [17] studied the importance of process parameters in the micro-grinding of hardened steel. Morgan et al.'s [18] study, specifically focused on cemented carbides, revealed that the specific energy was initially high at the onset of tool-workpiece contact, but rapidly decreased to an almost constant value of 500 J/mm^3 after a stable tool engagement. Huang and Kuriyagawa [19] performed grinding of cemented carbide used for mold inserts, achieving better form accuracy and surface roughness even though they found small chipping of the material.

Based on the previous research, it has been observed that critical issues such as high rotational speeds, significant tool deflection, uneven grit protrusion, varying bond layer thickness, rapid tool wear, sensitivity to runout resulting in vibrations, and excessive tool loading are encountered [20]. While challenges such as wear and deflection can be addressed by optimizing grinding parameters, it was recognized that more research is needed, particularly in the areas of cooling and lubrication, and the investigation of vitrified pins, as most studies have focused primarily on electroplated (single layer) tools. In summary, research on pin grinding, particularly for cemented carbide materials, remains limited. Given this knowledge gap, the objective of the present study is to investigate the effects of various cooling-lubrication methods, including dry machining conditions as an extreme reference, on the grinding of cemented carbide using a vitrified diamond grinding pin. A secondary objective is to investigate the wheel-loading phenomena associated with different cooling-lubrication methods. The insights gained from this research could provide valuable information for future efforts to extend these experiments to conventional grinding applications using LCO_2.

1 EXPERIMENTAL

Pin grinding experiments were conducted using the Sodick MC 430L high-speed milling machine, The employed grinding tool was a vitrified-bonded diamond pin (D32-46-150-V-3195) mounted on a tungsten-carbide shaft, produced by Meister Abrasives. The pin had a diameter of 6 mm. The workpiece material chosen was an uncoated cemented carbide blank (GC1130 grade), designed for a gear-cutting insert and fabricated from the fine-grained, high-chromium by Sandvik Coromant. This workpiece, with dimensions of 85 mm × 15 mm × 13 mm, was subject to hardness testing with a Vickers microhardness tester, yielding a hardness value of

79 HV. Fig. 1 shows images of both the tool and the workpiece utilized in the grinding experiments.

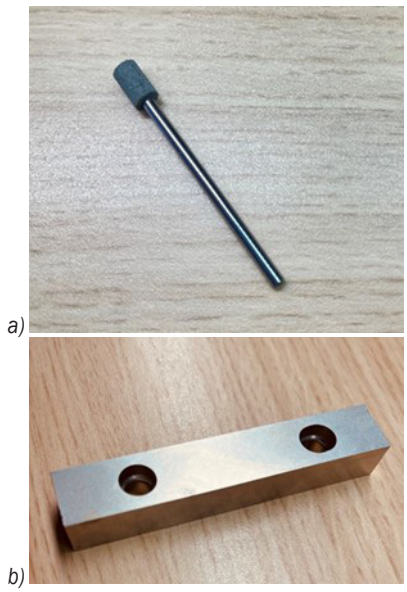

Fig. 1. **a**) *Diamond grinding tool, and b) cemented carbide workpiece*

After each test, the grinding wheel underwent a conditioning and cleaning process using a hand-sticking method with a fine-grit mesh silicon-carbide stone. The grinding experiments consisted of five varying grinding wheel speeds, ranging from 4 m/s to 12 m/s, while maintaining a constant workpiece speed (100 mm/min) and depth of cut (10 µm). This range in grinding wheel speeds provided six distinct grinding aggressiveness conditions. Table 1 lists the utilized grinding parameters and the corresponding calculated aggressiveness numbers, *Aggr*.

Table 1. *Grinding parameters used in the experiments*

Experiment no.	Wheel speed [m/s]	Workpiece speed [mm/min]	Depth of cut [μm]	*Aggr* [-]
1	12	100	10	5.68
2	10	100	10	6.82
3	8	100	10	8.52
4	6	100	10	11.36
5	4	100	10	17.04

Fig. 2 illustrates the experimental setup used for this study. A Kistler Type 9129AA dynamometer was employed to measure the normal and tangential grinding forces. During the LCO_2-MQL trials, the dynamometer was insulated to minimize potential drift and bias in force readings stemming from the low-temperature effects on the piezoelectric dynamometer. To assure the reliability and reproducibility of the results, each experimental test was replicated four times.

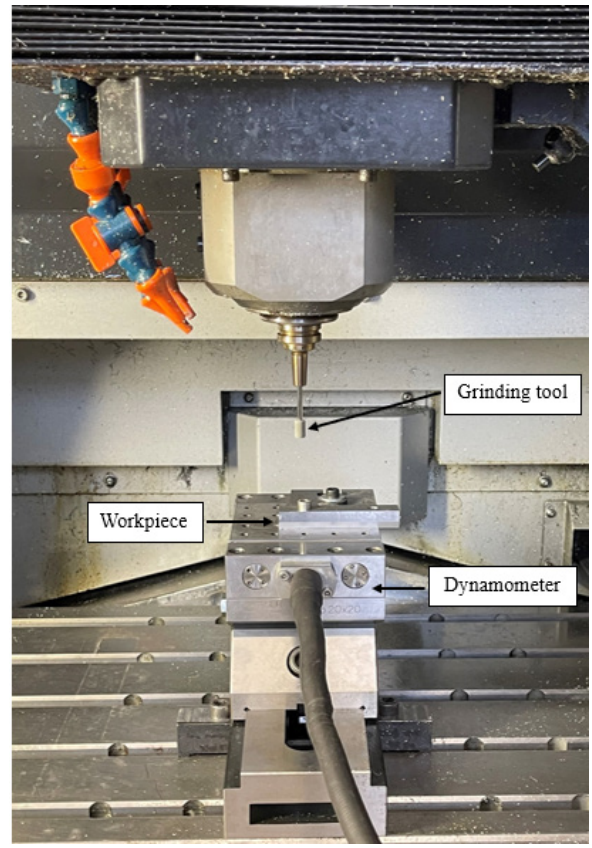

Fig. 2. *Experimental setup*

The tool's topography following each experiment was initially assessed utilizing a Keyence VHX 6000 digital microscope. Furthermore, an FEI/Philips XL30 ESEM (Environmental Scanning Electron Microscope) was employed to examine wheel surface and ascertain potential wheel loading or clogging issues.

Three different cooling-lubrication conditions were utilized in the grinding experiments: dry, emulsion, and LCO_2-MQL grinding. For "emulsion grinding" a conventional water-based cutting fluid in the form of a soluble oil emulsion with a concentration of 6 % was employed. The LCO_2-MQL system deployed, ArcLub One, was developed at the University of Ljubljana, Slovenia. This novel cooling-lubrication approach involves a single-channel supply of a pre-mixed blend of LCO_2 and oil, conveyed as MQL. As nonpolar oils, which are completely soluble in LCO_2, lead to smaller oil droplet sizes and more uniform distribution in MQL, a low-viscosity,

nonpolar oil was selected as the lubricant [11] and [21]. The chosen lubricant was HAROLBIO 0, a petroleum-free, saturated synthetic ester with a viscosity index of 152 (ASTM D 2270). An external nozzle was used to deliver the cooling lubricant to the grinding zone.

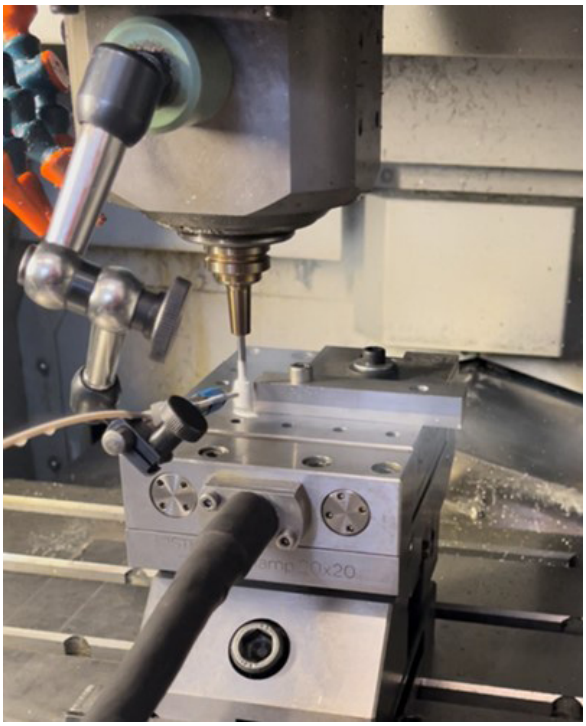

Fig. 3. *LCO_2-MQL grinding set up*

2 RESULTS AND DISCUSSION

In this section, an analysis of the results is presented, focusing on the evaluation of the grinding process through grindability aspects such as grinding forces, grinding force ratios, grinding specific energy, wheel loading, and wheel topography. The significance and novelty of the results are discussed. Limitations associated with the techniques used and the results presented are also highlighted.

2.1 Grinding Forces

The normal and tangential grinding forces were measured across four repetitions. Since the measured grinding forces remained relatively constant across these repetitions, average grinding force values were used in Figs. 4 and 5 to show their variation with *Aggr* and cooling-lubrication conditions. Both tangential and normal grinding forces were found to decrease with an increase in cutting speed – an expected result given that higher cutting speeds yield smaller *Aggr* values. In all cases, normal forces exceeded tangential grinding forces, an observation commonly noted in conventional grinding operations as well.

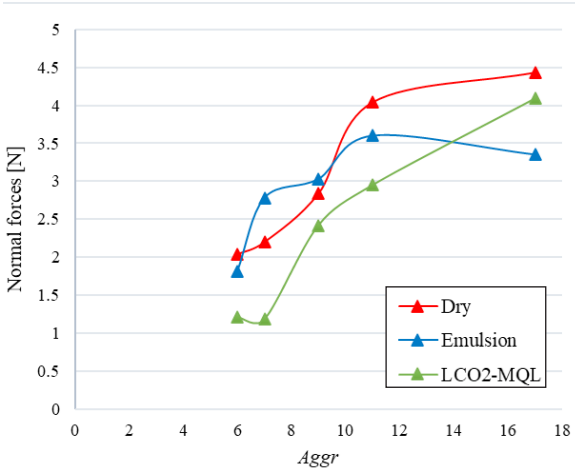

Fig. 4. *Normal grinding forces vs. Aggr*

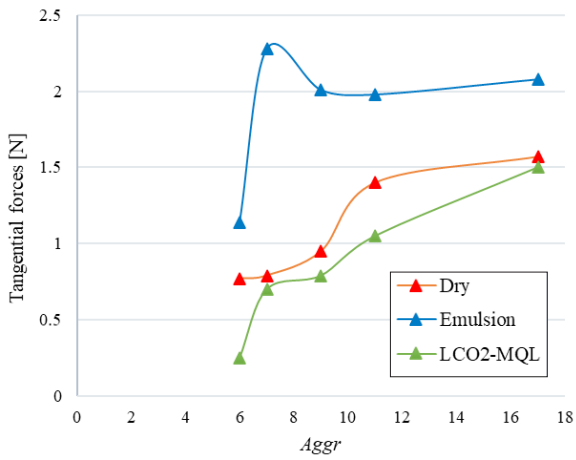

Fig. 5. *Tangential grinding forces vs. Aggr*

The normal grinding forces are lower in LCO_2-MQL grinding for the first five experiments and range from 1.2 N to 4.09 N, followed by emulsion and dry grinding. The tangential grinding forces are also lower for LCO_2-MQL grinding and range from 0.25 N to 1.5 N, followed by dry and emulsion grinding. The grinding force values were found to be exceptionally high in the last experiments of emulsion and LCO_2-MQL grinding due to excessive wheel wear and wheel loading. The sixth experiment at the highest *Aggr* is clearly an outlier, and hence not a representative case of normal grinding conditions. The normal and tangential grinding forces are comprised of two components, one due to cutting and one due to sliding on the wear flats [22]. The low tangential grinding forces observed in LCO_2-MQL grinding indicate

efficient shear in the grinding zone and lubrication. A boundary-lubricating film was likely formed through polar group adsorption [11]. The lubricating film allows the oil to penetrate the grinding zone, which helps to prevent issues such as evaporation, and adhesion that can occur due to high temperatures, when the lubricant layer is sufficiently thick, it provides an effective lubrication effect, further reducing grinding forces [23]. Hence, the combined effect of LCO_2 and MQL can enhance the formation of the lubricating film. This combination facilitates a continuous lubrication effect, which contributes to the reduction of grinding forces and friction [24]. The grinding forces are higher under dry grinding because of the excessive sliding and plowing action [25]. One can also observe very steady levels of normal and tangential forces in LCO_2-MQL, which indicate minimal tool wear, until its collapse [26] at excessive (Experiment 6) grinding condition at the highest tested *Aggr*.

The grinding force ratio is further analyzed as it provides indirect information regarding the efficiency of the grinding process. It can characterize the lubrication effect at the wheel/workpiece interface. A high grinding force ratio suggests poor lubrication in the grinding zone, whereas improved lubrication corresponds to a lower force ratio. The force ratio in grinding is synonymous with the coefficient of friction between sliding surfaces. For hard materials, the coefficient of friction is high, indicating worse grindability [27]. The following expression is used to calculate the grinding force ratio:

$$\mu = F_T / F_N, \quad (1)$$

where F_T is the tangential grinding force, and F_N is the normal grinding force.

Fig. 6 shows the grinding force ratios under varying cooling-lubrication conditions. The grinding force ratios for dry grinding range from 0.32 to 0.38. In comparison, grinding with emulsion gives ratios between 0.50 and 0.82, representing an increase of 56 % to 116 % compared to dry grinding. On the other hand, LCO_2 shows the lowest force ratios, ranging from 0.21 to 0.37, representing a 3 % to 34 % decrease compared to dry grinding and a 55 % to 58 % decrease compared to emulsion grinding. The grinding force ratio is maximum under emulsion grinding followed by dry grinding. The grinding force ratio in LCO_2-MQL grinding is lower compared to that in dry and emulsion grinding, indicating that the grindability, with respect to friction in the grinding zone, is enhanced with LCO_2-MQL grinding. The penetration of LCO_2-MQL into the grinding zone creating a boundary lubrication layer provides better lubrication, hence reducing friction [23].

2.2. Specific Grinding Energy

Specific grinding energy, u, is a fundamental parameter for gauging the efficiency of the grinding process. This quantity is defined as the energy expended per unit volume of material removed [28]. Specific energy is dependent on the tangential grinding force, the employed grinding parameters, the workpiece material's grindability, the tool's topography, and the tribological conditions in the grinding zone, which are largely determined by the cooling-lubrication method

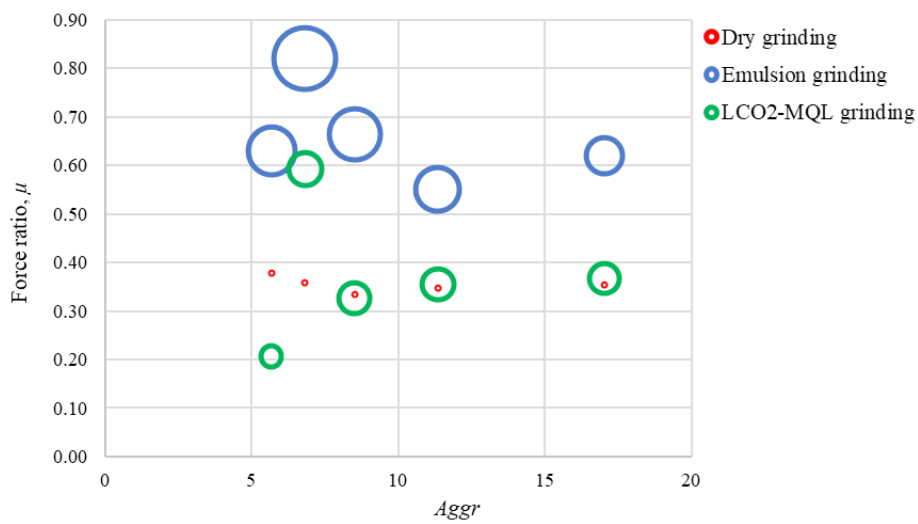

Fig. 6. *Grinding force ratios vs. Aggr*

used. The following equation can be used to calculate the specific energy [28]:

$$u = F_T V_s / (V_w a b) \quad (2)$$

where F_T is the tangential grinding force, V_s is the wheel speed, V_w is the workpiece speed, a is the depth of cut, and b is the grinding width of cut.

Badger et al. [29] introduced the dimensionless aggressiveness number, *Aggr*, a fundamental parameter encapsulating the geometry and kinematics of a grinding process. In this study, *Aggr* was therefore used to quantify the intensity of abrasive interaction during the experiments as it is fundamentally linked to the specific grinding energy. As such, the outcomes of the pin-grinding experiments were analyzed and charted across various aggressiveness numbers. The aggressiveness number can be calculated as follows:

$$Aggr = 10^6 (V_w / V_s) (a / d_s)^{1/2}, \quad (3)$$

where d_s is the diameter of the wheel.

The obtained specific grinding energy values for the different cooling-lubrication methods are given in Table 2. The specific energies here were calculated using the measured tangential grinding forces at different *Aggr* values. The specific grinding energy was lower at higher *Aggr*, indicating that increasing the wheel speed improves the efficiency of material removal, since the lower specific energy indicates lower proportions of sliding/friction in the chip formation process [3]. This phenomenon is especially noticeable in pin-grinding or when the depth of cut is very small.

Table 2. *Specific grinding energy values for different cooling-lubrication conditions*

Experiment No.	*Aggr* [-]	Specific energy [J/mm³]		
		Dry	Emulsion	LCO_2-MQL
1	5.68	55	82	18
2	6.82	47	137	42
3	8.52	45	96	38
4	11.36	50	71	38
5	17.04	37	50	36

In LCO_2-MQL grinding, the obtained specific energy values range from 18 J/mm³ to 42 J/mm³, the lowest among the tested cooling-lubrication conditions. By comparison, the values for dry grinding are between 37 J/mm³ and 55 J/mm³, and for emulsion grinding, they span from 50 J/mm³ to 137 J/mm³. These results suggest that LCO_2-MQL cooling lubrication enables the most efficient cutting.

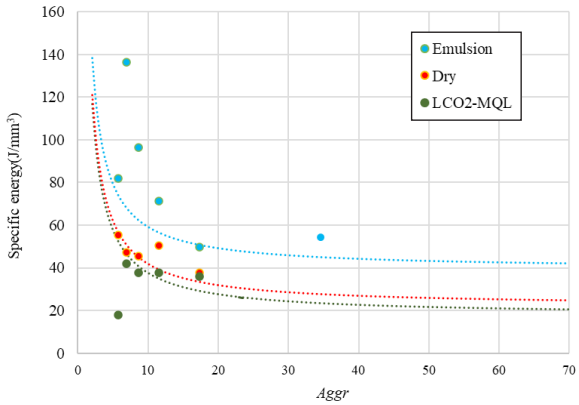

Fig. 7. *Specific grinding energy vs. Aggr*

The specific energy curve depicted in Fig. 7 exhibits a typical size effect, indicating that specific energy declines as the aggressiveness number (or undeformed chip thickness) increases. This effect can be attributed to the transitional nature of the grinding process among the sliding, ploughing, and cutting regimes. With larger *Aggr* values, the grinding process is dominated by the cutting regime, where material removal occurs predominantly through shearing. Conversely, at lower *Aggr* values, the grits of the grinding wheel largely slide across the workpiece surface, resulting in limited material removal. The latter behavior necessitates a greater energy expenditure to remove a unit volume of material, thereby contributing to the observed size effect.

2.3 Wheel Topography

After each experiment, regardless of the cooling-lubrication method utilized, wheel loading was noted; a phenomenon expected due to the low grinding aggressiveness. The tested *Aggr* values in pin-grinding with a diamond pin are significantly smaller compared to values observed in larger-scale grinding operations. This is mentioned, as the problem of wheel loading is also common in conventional grinding of cemented carbides, particularly when using straight oil as a grinding fluid. This issue was mitigated during the sequence of experiments and their repetitions by conducting a thorough conditioning and cleaning of the grinding wheel surface after each trial using an abrasive stone/stick, as described in Section 1. Figs. 8 to 10 depict images of the wheel topography following grinding under different cooling-lubrication conditions. With dry grinding (Fig 8), the wheel loading is clearly visible after each experiment. This is due to the lack of grinding fluid to flush away the

chips during grinding and to reduce temperatures. In emulsion grinding, the wheel loading is less than in other methods due to the effectiveness of the emulsion in preventing clogging and removing chips. However, LCO_2-MQL grinding (Fig. 10) presents a stark contrast. Although LCO_2-MQL has the lowest values of grinding forces and specific energy, it has a substantial wheel loading, which is noteworthy. This is likely due to the lack of oxygen in a CO_2 atmosphere, which may enhance the adhesion of metal particles (chips) to the grinding wheel.

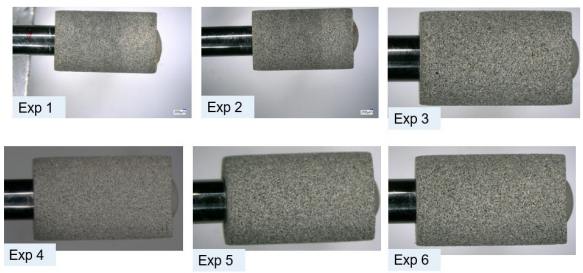

Fig. 8. *Wheel loading after dry grinding*

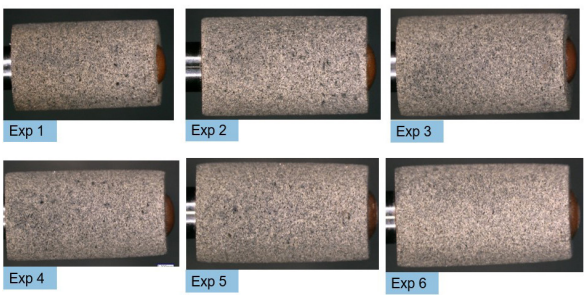

Fig. 9. *Wheel loading after grinding with emulsion*

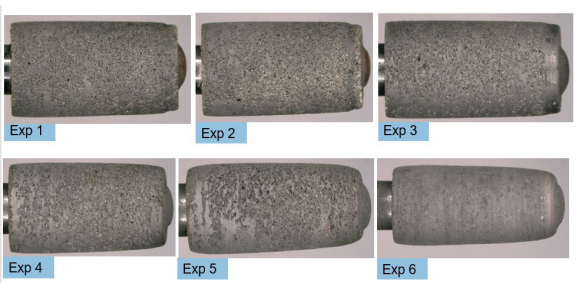

Fig. 10. *Wheel loading after LCO_2-MQL grinding*

To investigate the loading for the LCO_2-MQL case more thoroughly, the pins were gold sputtered before electron back-scatter diffraction pattern analysis was conducted. Fig. 11 displays scanning electron micrographs (Fig. 11a) magnification 350 x, Fig. 11b) magnification 95 x), which reveal the particles loaded onto the wheel. The bright white, shiny areas represent the cemented carbide materials loaded into the wheel, a conclusion further supported by a chemical analysis of the wheel surface. This result could be due to inefficient chip evacuation when using LCO_2-MQL, which contradicts previous findings of reduced loading during LCO_2-MQL grinding of a titanium alloy with a conventional wheel [30].

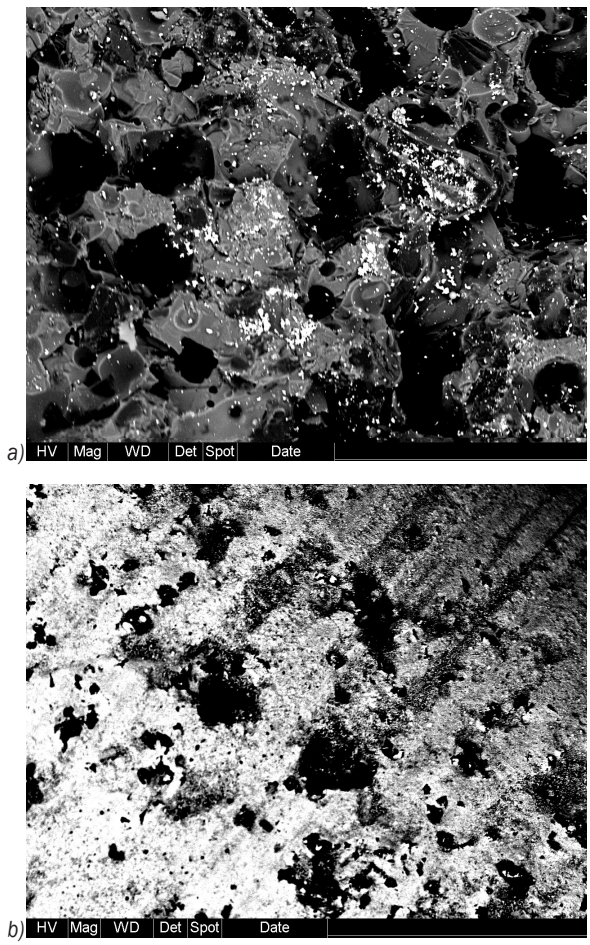

Fig. 11. *ESEM images of the wheel surface after LCO_2-MQL grinding; a) ESEM (magnification 350×), and b) ESEM (magnification 95×)*

While the presence of oxygen in a typical grinding atmosphere minimizes the sticking, or "adhesion," of metal particles to each other and to the workpiece, enhancing the overall grinding process, its absence in environments like a vacuum or an inert (non-reactive) atmosphere can significantly alter the process. Specifically, the lack of oxygen may increase the likelihood of metal particles sticking to each other and adhering to the workpiece and the grinding wheel [31] and [32]. When oxygen is absent, freshly created metal workpiece particles, or chips, with pristine, uncontaminated surfaces, have a propensity to physically stick to one another and to the wheel

surface. This behavior subsequently leads to the loading and clogging of the wheel [28].

3 CONCLUSIONS

In conclusion, this study was conducted to advance the understanding of the effects of varying cooling-lubrication conditions on pin grinding of cemented carbides. Through the detailed investigation of three different conditions: LCO_2-MQL, dry, and emulsion grinding – the following results were obtained.

The grinding forces and specific grinding energies were found to be lowest in LCO_2-MQL grinding. It was found that grinding under emulsion (flood) conditions resulted in a poorer performance compared to dry grinding.

In addition, the lack of oxygen in a CO_2 atmosphere can potentially increase the adhesion of metal particles (chips) to the grinding wheel, leading to challenges in the grinding process, especially severe wheel loading in the case of LCO_2-MQL grinding. However, the novel method of cooling-lubrication, using lubricated liquid carbon dioxide, while demonstrating a wheel loading problem, showed potential for improved grinding efficiency.

These findings pave the way for further investigation into optimizing the material removal processes in the pin-grinding of cemented carbides, with a particular focus on addressing wheel loading issues and understanding the role of the grinding atmosphere.

4 ACKNOWLEDGEMENTS

The authors would like to express their gratitude to Meister Abrasives and Sandvik Coromant for their invaluable support in this research endeavor. Special appreciation is extended to Mr. Elias Navarro and Mr. Per Norlin for providing the vitrified diamond pins and cemented carbide blanks, respectively. Further, we acknowledge the financial support received from the Slovenian Research Agency (No. 54942. Lastly, partial support from the EIT Manufacturing program, through the project (21193: Transitioning to a Waste-free Production – International Cryogenic + MQL Machining Activity), is gratefully recognized.

5 REFERENCES

[1] Hegeman, J.B.J.W., de Hosson, J.Th.M., de With, G. (2001). Grinding of WC-Co hardmetals. *Wear*, vol. 248, no. 1-2, p. 187-196, **DOI:10.1016/s0043-1648(00)00561-5**.

[2] Mahata, S., Mukhopadhyay, M., Kundu, A., Banerjee, A., Mandal, B., Das, S. (2020). Grinding titanium alloys applying small quantity lubrication. *SN Applied Sciences*, vol. 2, no. 2, **DOI:10.1007/s42452-020-2792-2**.

[3] Kadivar, M., Daneshi, A., Azarhoushang, B. (2018). Study of specific energy in grinding of tungsten carbide. XIVth International Conference on High-Speed Machining.

[4] Badger, J. (2015). Grinding of sub-micron-grade carbide: Contact and wear mechanisms, loading, conditioning, scrubbing, and resin-bond degradation. *CIRP Annals*, vol. 64, no. 1, p. 341-344, **DOI:10.1016/j.cirp.2015.04.007**.

[5] Dražumerič, R., Badger, J., Klement, U., Krajnik, P. (2018). Truing of diamond wheels - Geometry, kinematics, and removal mechanisms. *CIRP Annals*, vol. 67, no. 1, p. 345-348, **DOI:10.1016/j.cirp.2018.04.091**.

[6] Koshy, P., Jain, V.K., Lal, G.K. (1997). Grinding of cemented carbide with electrical spark assistance. *Journal of Materials Processing Technology*, vol. 72, no. 1, p. 61-68, **DOI:10.1016/S0924-0136(97)00130-1**.

[7] Krajnik, P., Rashid, A., Pušavec, F., Remškar, M., Yui, A., Nikkam, N., Toprak, M.S. (2016). Transitioning to sustainable production - part III: Developments and possibilities for integration of nanotechnology into material processing technologies. *Journal of Cleaner Production*, vol. 112, p. 1156-1164, **DOI:10.1016/j.jclepro.2015.08.064**.

[8] Hosseini, S.F., Emami, M., Sadeghi, M.H. (2018). An experimental investigation on the effects of minimum quantity nano lubricant application in grinding process of Tungsten carbide. *Journal of Manufacturing Processes*, vol. 35, p. 244-253, **DOI:10.1016/j.jmapro.2018.08.007**.

[9] Pušavec, F., Grguraš, D., Koch, M., Krajnik, P. (2019). Cooling capability of liquid nitrogen and carbon dioxide in cryogenic milling. *CIRP Annals*, vol. 68, no. 1, p. 73-76, **DOI:10.1016/j.cirp.2019.03.016**.

[10] Laakso, V.A.S., Mallipeddi, D., Krajnik, P. (2022). Evaluation of subcooled MQL in CBN hard turning of powder-based Cr-Mo-V tool steel using simulations and experiments. *The International Journal of Advanced Manufacturing Technology*, vol. 118, p. 511-531, **DOI:10.1007/s00170-021-07901-x**.

[11] Grguraš, D., Sterle, L., Krajnik, P., Pušavec, F. (2019). A novel cryogenic machining concept based on lubricated liquid carbon dioxide. *International Journal of Machine Tools and Manufacture*, vol. 145, art. ID 103456, **DOI:10.1016/j.ijmachtools.2019.103456**.

[12] Sterle, L., Krajnik, P., Pušavec, F. (2021). The effects of liquid-CO_2 cooling, MQL, and cutting parameters on drilling performance. *CIRP Annals*, vol. 70, no. 1, p. 79-82, **DOI:10.1016/j.cirp.2021.04.007**.

[13] Pušavec, F., Sterle, L., Kalin, M., Mallipeddi, D., Krajnik, P. (2020). Tribology of solid-lubricated liquid carbon dioxide assisted machining. *CIRP Annals*, vol. 69, no. 1, p. 69-72, **DOI:10.1016/j.cirp.2020.04.033**.

[14] Aguirre, F.M., Gonzalez, L.S., Hood, R., Kong, M.C., Novovic, D., Soo, L.S. (2023). Assessment of advanced process configurations for improving workpiece surface finish in point grinding. *CIRP Annals*, vol. 72, no. 1, p. 267-272, **DOI:10.1016/j.cirp.2023.04.078**.

[15] Kadivar, M., Azarhoushang, B., Shamray, S., Krajnik, P. (2018). The effect of dressing parameters on micro-grinding of titanium alloy. *Precision Engineering*, vol. 51, p. 176-185, **DOI:10.1016/j.precisioneng.2017.08.008**.

[16] Kadivar, M., Azarhoushang, B., Klement, U., Krajnik, P. (2021). The role of specific energy in micro-grinding of titanium alloy. *Precision Engineering*, vol. 72, p. 172-183, **DOI:10.1016/j.precisioneng.2021.04.015**.

[17] Arrabiyeh, A.P., Setti, D., Basten, S., Kirsch, B., Aurich, C.J. (2019). Micro grinding 16MnCr5 hardened steel using micro pencil grinding tools with diameters ~ 50 mm. *CIRP Journal of Manufacturing Science and Technology*, vol. 27, p. 1-10, **DOI:10.1016/j.cirpj.2019.10.002**.

[18] Morgan, J.C., Vallance, R.R., Marsh, R.E. (2007). Specific grinding energy while micro grinding tungsten carbide with polycrystalline diamond micro tools. *ICOMM*.

[19] Huang, H., Kuriyagawa, T. (2005). Effect of microstructure on material removal mechanisms in nano/micro grinding of tungsten carbide mould inserts. *International Conference on Leading Edge Manufacturing in 21st Century*, p. 877-882, **DOI:10.1299/jsmelem.2005.2.877**.

[20] Pietrowa, N., Curtis, D., Ghadbeigi, H., Novovic, D., McGourlay, J. (2021). An investigation into the challenges of the point grinding machining process. *Procedia CIRP*, vol. 101. p. 190-193, **DOI:10.1016/j.procir.2020.09.19**5.

[21] Grguraš, D., Sterle, L., Kastelic, L., Courbon, C., Pušavec, F. (2021). Media flow analysis of single-channel pre-mixed liquid CO2 and MQL in sustainable machining. *Strojniški vestnik - Journal of Mechanical Engineering*, vol. 67, no. 1-2, p. 3-10, **DOI:10.5545/sv-jme.2020.7076**.

[22] Macerol, N., Franca, F.P.L., Drazumeric, R., Krajnik, P. (2022). The effects of grit properties and dressing on grinding mechanics and wheel performance: Analytical assessment framework. *International Journal of Machine Tools and Manufacture*, vol. 180, art. ID 103919, **DOI:10.1016/j.ijmachtools.2022.103919**.

[23] Liu, M., Li, C., Yang, M., Gao, T., Wang, X., Cui, X., Zhang, Y., Said, Z., Sharma, S. (2023). Mechanism and enhanced grindability of cryogenic air combined with bio lubricant grinding titanium alloy. *Tribology International*, vol. 187, art. ID 108704, **DOI:10.1016/j.triboint.2023.108704**.

[24] Garcia, E., Pombo, I., Sanchez, A.J., Ortega, N., Izquierdo, B., Plaza, S., Marquinez, I., J., Heinzel, C., Mourek, D. (2013). Reduction of oil and gas consumption in grinding technology using high pour-point lubricants. *Journal of Cleaner Production*, vol. 51, p. 99-108, **DOI:10.1016/j.jclepro.2013.01.037**.

[25] Prashanth, S.G., Sekar, P., Bontha, S., Balan, A.S.S. (2022). Grinding parameters prediction under different cooling environments using machine learning techniques. *Materials and Manufacturing Processes*, vol. 38, no. 2, p. 235-244, **DOI:10.1080/10426914.2022.2116043**.

[26] Badger, J. (2009). Factors affecting wheel collapse in grinding. CIRP Annals, vol. 58, no.1, p. 307-310, **DOI:10.1016/j.cirp.2009.03.048**.

[27] Wu, W., Li, C., Yang, M., Zhang, Y., Jia, D., Hou, Y., Li, R., Cao, H., Han, Z. (2019). Specific energy and G ratio of grinding cemented carbide under different cooling and lubrication conditions. *The International Journal of Advanced Manufacturing Technology*, vol. 105, p. 67-82, **DOI:10.1007/s00170-019-04156-5**.

[28] Malkin, S., Guo, C. (2008). *Grinding Technology: Theory and Applications of Machining with Abrasives: Second Edition*, Industrial Press, Inc., New York.

[29] Badger, J., Dražumerič, R., Krajnik, P. (2021). Application of the dimensionless Aggressiveness number in abrasive processes. *Procedia CIRP*, vol. 102, p. 361-368, **DOI:10.1016/j.procir.2021.09.062**.

[30] Singh, S.K., Jha, A.K., Ray, A., Dewangan, S. (2022). Enhancing grinding parameters of TC4 titanium superalloy by using a hybrid eco-friendly cooling system. *Materials Today*, vol. 62, no. 3, p. 1505-1509, **DOI:10.1016/j.matpr.2022.02.214**.

[31] Duwell, E.J., Hong, I.S., McDonald, W.J. (1969). The effect of oxygen and water on the dynamics of chip formation during grinding. *A S L E Transactions*, vol. 12, no. 1, p. 86-93, **DOI:10.1080/05698196908972250**.

[32] Outwater, J.O., Shaw, M.C. (1952). Surface Temperatures in Grinding. *ASME Journal of Fluids Engineering*, vol. 74, no. 1, p. 73-81, **DOI:10.1115/1.4015689**.